Available online at www.sciencedirect.com

ScienceDirect

Geochimica et Cosmochimica Acta 126 (2014) 455–474

Geochimica et Cosmochimica Acta

www.elsevier.com/locate/gca

Biogeochemical implications from dissolved rare earth element and Nd isotope distributions in the Gulf of Alaska

Brian A. Haley [a,*], Martin Frank [b], Ed Hathorne [b], Nick Pisias [a]

[a] CEOAS, 104 CEOAS Admin. Bldg., Corvallis, OR 97331-5503, USA
[b] GEOMAR Helmholtz Centre for Ocean Research Kiel, Wischhofstraße 1-3, 24148 Kiel, Germany

Received 13 March 2013; accepted in revised form 9 November 2013; Available online 22 November 2013

Abstract

Dissolved rare earth element (REE) concentrations and Nd isotope compositions were measured for surface waters and full water column profiles of the Gulf of Alaska (GoA), and compared to water mass properties and circulation in order to better understand the mechanisms controlling the input and transport of REEs in the ocean. The REEs display a typical open-ocean range of concentrations (i.e., La: 12–66 pM; Lu: 0.2–2.5 pM) and depth distributions (i.e., surface ocean depletion and enrichment with water depth). Nd isotope signatures are highly radiogenic, as expected for the North Pacific margin (ranging from −3.8 to +0.2 εNd). The most radiogenic values were found in the coastal waters but also in the cores of eddies, indicating efficient export of REEs from the margins and across the mixed layer. This is the first time that distinct Nd isotope distributions in near surface waters can be directly assigned to offshore eddy transport. A distinct mid-depth (~2200 m) Nd isotope signal was found that most likely reflects advection of a water mass that formed through past down-welling in the Northern Pacific. Subsurface Nd isotope compositions appear to behave conservatively and can be explained through a REE distribution model proposed here. This model is based on multivariate analysis of the REEs and invokes two distinct "pools" of dissolved REEs: a "passive pool" complexed by carbonate ions, and a "bio-reactive pool" that is microbially manipulated. The latter "pool" is only significant in the upper water column and most likely reflects the indirect effects of microbial cycling of iron. Our model of the open ocean REE distribution contributes to explaining the conservative nature of Nd isotopes and provides a mechanism linking surface ocean and pore water REE dynamics.
© 2013 Elsevier Ltd. All rights reserved.

1. INTRODUCTION

1.1. Background

The rare earth elements (REEs) are a coherent series of elements that share chemical properties due to similar outer electron configuration, but whose abundances are fractionated during environmental processes because of the so-called "lanthanide contraction" across the series (e.g., reviews of Elderfield, 1988; Byrne and Sholkovitz, 1996). This fractionation can be used to trace and understand environmental processes. In the oceans, the dissolved REEs show "scavenged element" water column characteristics, which are thought to reflect adsorption–desorption reactions between dissolved REEs and particulate matter (Sholkovitz et al., 1994). In detail, the nature of these interactions is not well known and largely based on relatively few analyses (e.g., Murphy and Dymond, 1984; Sholkovitz et al., 1994; Alibo and Nozaki, 1999; Akagi et al., 2011) and models (Jones et al., 2008; Siddall et al., 2008; Arsouze et al., 2009; Rempfer et al., 2011). For example, while a role for organic matter in REE biogeochemistry has been hypothesized, organic–REE interactions are not well-constrained (Haley et al., 2004; Takahashi et al., 2005; Sonke and Salters, 2006; Ngwenya et al., 2010). As an example, while there is, as yet, no known biological function of the REEs, biological mediation plays a strong role in marine cerium (Ce) redox chemistry (Moffett,

* Corresponding author. Tel.: +1 5417372649.
E-mail address: bhaley@coas.oregonstate.edu (B.A. Haley).

0016-7037/$ - see front matter © 2013 Elsevier Ltd. All rights reserved.
http://dx.doi.org/10.1016/j.gca.2013.11.012

1990). Finally, the geochemical properties of REEs as inferred from water column data have yet to be fully reconciled with the chemical behavior of REEs in marine pore waters, which has been argued to reflect the final reversal of processes occurring in the overlying water column (Haley et al., 2004). These observations and others, including uncertainties on the fundamental REE oceanic input function (Haley and Klinkhammer, 2003; Lacan and Jeandel, 2005; Jeandel et al., 2007; Johannesson and Burdige, 2007), make it clear that even after over 40 years of research (Goldberg et al., 1963), much is left to be learned about the behavior of REEs in the oceans and the information they can provide on oceanic biogeochemical processes.

The dissolved radiogenic isotope composition of neodymium (Nd), one of the Light REEs (LREEs), is of particular interest to oceanographers and paleoceanographers as a tracer of deep ocean circulation. A deep-ocean residence time of Nd less than the global mixing time of deep water in the modern ocean means that Nd isotopic compositions can be used as a "quasi-conservative" tracer of ocean circulation and water mass mixing, particularly at a distance from external inputs (Frank, 2002; Goldstein and Hemming, 2003). However, this concept is partly inconsistent because Nd as an element behaves non-conservatively and is clearly involved in chemical and physical water column processes, as described above. This dichotomy has been referred to as the "Nd paradox" (Tachikawa et al., 1999; Goldstein and Hemming, 2003; Siddall et al., 2008). The fundamental resolution of the "Nd paradox" lies in a better understanding of the REEs and Nd isotopes in the water column, which can only be achieved through paired analyses in differing ocean environments (such as in the framework of the international GEOTRACES program; Henderson et al., 2007). Here, we present the first combined dissolved distributions of REEs and Nd isotopes in the Gulf of Alaska. These data indicate that while the behavior of REEs and Nd isotopes in the open and, in particular, the deeper ocean is fairly well understood, there are still large gaps in knowledge on the processes controlling surface and marginal ocean REE and Nd isotope distributions and inputs.

1.2. Study area

The upper ocean circulation in the Gulf of Alaska (GoA) can be simplified as a system of two major currents surrounding the large cyclonic Alaska gyre (Fig. 1; Ladd et al., 2009). The coastal currents are the Alaska current (AlC) in the eastern part and the Alaskan Stream (AlS) in the northern and northwestern parts of the GoA. Subsurface water mass characteristics in the GoA are somewhat different from those generally observed in the North Pacific (Talley et al., 2011). In particular, a thermal minimum can occur, supported by a strong halocline in winter months, known as Dichothermal Water (DtW; Miura et al., 2002), clearly discerned by a shallow-water T-S inflection near 100 m water depth (Fig. 2). Moreover, DtW is expected to be highly oxygenated in summer (Talley et al., 2011), borne-out by significantly elevated oxygen concentrations between 30 and 100 m depth during our cruise (not shown). Thus, we infer that the residue of DtW were still present during late summer when our cruise took place. Beneath DtW, a subsurface temperature maximum (~130 m water depth) was observed (Fig. 2), corresponding to the so-called

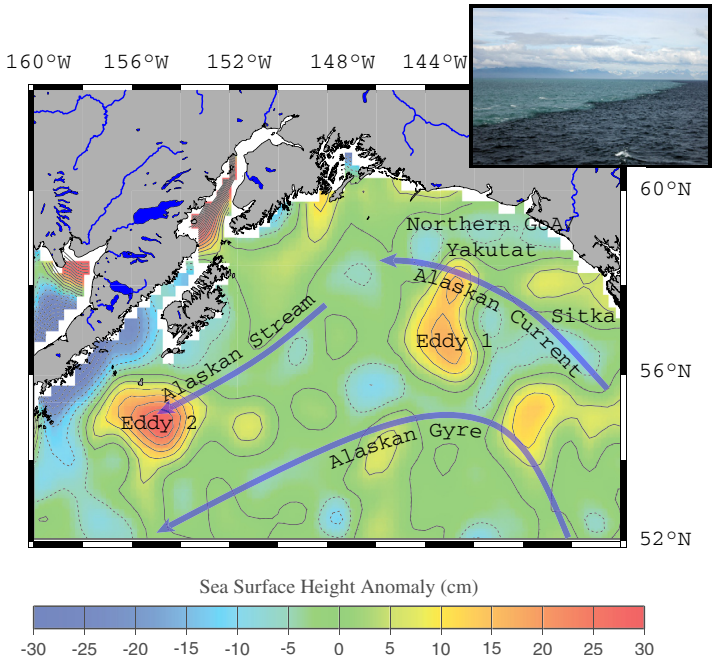

Fig. 1. Gulf of Alaska hydrography. Major surface currents shown with blue arrows (Talley et al., 2011). The locations of the Alaskan Gyre and both Yakutat and Sitka eddy source regions are demarcated. Sea surface height anomaly (from CCAR, University of Colorado) at a midpoint of the cruise period illustrates the two large eddies sampled. The surface current directions show that the motion of eddies is largely east to west across the GoA. *Inset picture* shows near-coastal water with high sediment load. (For interpretation of the references to color in this figure legend, the reader is referred to the web version of this article.)

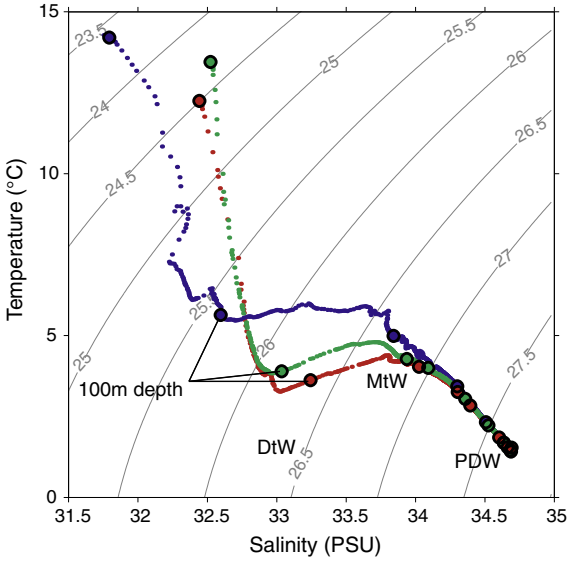

Fig. 2. Temperature–salinity data. T (°C) and Salinity (PSU) data from Profile 1 (red), 2 (green) and 4 (blue) (Profile 3 not shown). Locations of profiles are shown in Fig. 3. Large circles indicate discrete bottle samples. The temperature inversion near 100 m water depth is characteristic of Dicothermal Water (DtW) (Talley et al., 2011). (For interpretation of the references to color in this figure legend, the reader is referred to the web version of this article.)

mesothermal water (MtW; Talley et al., 2011). This water mass has been suggested to contain a strong laterally advected component originating from the east or south in order to explain its thermal isolation from the overlying DtW (Talley et al., 2011). Below 150 m water depth, the GoA is dominated by Pacific Deep Water (PDW), which is thought to form internally in the Pacific Ocean from a slowly diffusing Southern Ocean source and without a significant contribution from regional deep water production (Talley, 2007). The "core" of PDW is found at depths of ~2–2.5 km in the GoA region (Talley, 2007). Neither North Pacific Intermediate Water (NPIW) nor Antarctic Intermediate Water (AAIW) could be identified in the GoA during our cruise.

Of particular importance for the near surface hydrography and the biogeochemical composition in the GoA region is the influence of meso-scale anticyclonic eddies that typically form along the southern Alaskan margin, and are thus referred to as Haida, Sitka or Yakutat eddies (Ladd et al., 2009; Nudds and Shore, 2011). These eddies are believed to have a large impact on the biogeochemistry of the surface and deeper water column, for example, through delivery of micronutrients such as iron to the High Nutrient Low Cholorophyll (HNCL) region of the central Alaska gyre (Ladd et al., 2005; Lippiatt et al., 2010; Brown et al., 2012). Two eddies were sampled during this cruise and were identified by pronounced sea surface height anomalies in the northeastern and southwestern GoA (Fig. 1; data from CCAR, University of Colorado).

2. METHODS/SAMPLES

2.1. Sample collection

Samples were collected with the *R/V Thompson* between August 19 and September 17, 2007. Sampling locations are shown in Fig. 3. Surface water was collected underway

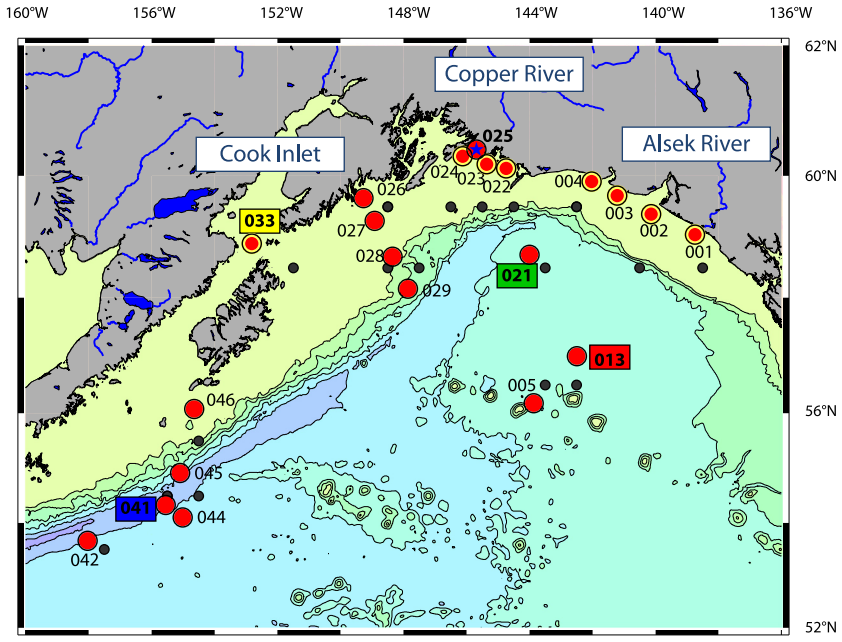

Fig. 3. Sample locations. Red dots: surface water samples; red dots labeled with numbers in boxes: full depth profile stations (red: Profile 1; green: Profile 2; yellow: Profile 3; blue: Profile 4); black dots: World Ocean Atlas (WOA '05) stations used for comparison; Blue star: Copper River sample location. Stations circled in yellow are surface samples that are classified as "passive" while all others are classified as "bioactive" (see text). Bathymetric lines represent 1 km intervals. (For interpretation of the references to color in this figure legend, the reader is referred to the web version of this article.)

using a towed "Fish sipper" system (Bruland et al., 2005). Pumping this water directly into a clean lab guaranteed trace metal clean sampling required, for example, for surface analyses of Fe concentrations. Four full depth water column profiles were also sampled using a rosette equipped with Niskin bottles. One sample (025) was collected by hand directly with clean 2 L bottles from off the side of a Zodiak raft within the Copper River "estuary" (i.e., in its lower-salinity mixing region behind barrier bars).

Except for sample 025, each sample represents ~20 L of water filtered through 0.45 μM filters using a high-flow peristaltic pump. Two liters were sub-sampled and separated immediately, acidified to pH ~2–2.5 with ultra-pure (quartz-distilled) 6 M HCl for analyses of REE concentrations. The remaining ~18 L of water, used for Nd isotopic analysis, were brought to pH ~2.5 with ultra-pure 6 M HCl, and ~100–150 mg of Fe added as a purified $FeCl_3$ solution. Once equilibrated, the water was brought to pH ~8–8.5 using ultra-pure ammonium hydroxide which led to precipitation of iron oxides that scavenged the dissolved REEs from the seawater. Most of the seawater was then siphoned-off and the remaining seawater and the Fe-precipitate were returned to the home laboratory.

2.2. Sample analyses

The REE concentrations were measured using a recently developed Online Preconcentration Inductively Coupled Plasma Mass Spectrometry (OP-ICP-MS) technique (Hathorne et al., 2012). This automated technique efficiently separates the major matrix elements and then allows direct injection of the pre-concentrated REEs into the spray chamber of the ICP-MS (Agilent 7500ce operated at GEOMAR). The REEs have been shown not to fractionate from each other during this procedure (Hathorne et al., 2012), as also confirmed by results that are consistent with other laboratories and methods as part of the intercalibration efforts of the international GEOTRACES program (van de Flierdt et al., 2012). The procedural blank of this method is <~100ppq and the external reproducibilities (2σ) for each REE concentration (50 runs of a seawater sample) are given with Tables 1 and 2 (see Hathorne et al., 2012 for details).

For Nd isotope analyses, the Fe-precipitates were rinsed with Milli-Q water, and organic molecules were destroyed using concentrated ultra-pure HNO_3. The samples were then prepared and run through two chromatographic columns to obtain pure Nd: an AG50-12X resin cation exchange column, and a HDEHP column for Nd separation from the other REEs (Pin and Zalduegui, 1997; van de Flierdt et al., 2012). The procedural blank for Nd isotopic analysis was negligible (<30 pg). The purified Nd solutions were measured on a Thermo Triton Thermal Ionization Mass Spectrometer (TIMS) operated at GEOMAR. The measured $^{143}Nd/^{144}Nd$ ratios were corrected for instrumental mass bias using $^{146}Nd/^{144}Nd = 0.7219$ using an exponential fractionation law, and normalized for offset from JNdi-1 using replicate analyses (based on an accepted $^{143}Nd/^{144}Nd = 0.512115$; Tanaka et al., 2000). Duplicate analyses were carried out whenever possible. The external reproducibility (2σ), determined from repeated measurements of an in-house standard, was 0.35 εNd units over the course of a year (this reproducibility was always worse than the internal error of individual measurements; εNd corresponds to the measured $^{143}Nd/^{144}Nd$ normalized to a CHondritic Uniform Reservoir (CHUR) value of 0.512638, multiplied by 10^4; Jacobsen and Wasserburg, 1980).

3. RESULTS

The results will be described in two sections: First the surface waters reflecting the upper mixed layer and including all the "towed Fish" samples, as well as the uppermost samples of the water column profiles will be discussed (i.e., all samples taken above 10 m depth; Table 1), which will be followed by the presentation of the water column profile data (Table 2).

3.1. Surface waters

3.1.1. Seawater Properties and eddy mixing

Ship-board hydrographic measurements (salinity, temperature) were compared to annually-averaged estimates from the World Ocean Atlas (WOA) 2005 database and the regional patterns are consistent in both data sets. The westward cooling of surface waters, the saltier gyre region and the river-plume salinity anomalies (especially at the Alsek and Copper River mouths) are clearly identifiable. One difference is that the Alaska Current (AlC) is more clearly seen in the ship's salinity data as a continuous, almost trapped, current that disperses around the Cook Inlet. During September and August high freshwater discharge rates from melting of the abundant local glaciers were observed (maximum flow on the Alsek river occurred between July and August; (Alsek R. station, USGS 1512900, data available from USGS online data repository; waterdata.usgs.gov/nwis), making the Alaska Current (AlC) more distinct in the hydrographic parameters during the time of the cruise. This observation is supported by the abrupt delineation of sediment-laden waters clearly visible over the narrow shelf along the eastern Alaskan shoreline (inset in Fig. 1) reflecting the input of glacial flour as a consequence of the high, generally diffuse, sediment flux from the coastal mountains. Generally, however, the surface water conditions found on the cruise were comparable to the data of WOA '05, indicating that the samples are representative of the average conditions in the GoA (Table 1).

We were able to sample two eddies during the cruise (Fig. 1), both in the core and "ahead of" the direction of eddy motion (although these eddies were both approaching the end of their "lifetimes" and were dissipating rather than actively moving). The impact of eddies on trace metals is largely seen in the uppermost water column and is transient in accordance with temperature and salinity constantly being re-equilibrated in the mixed layer (Ladd et al., 2009; Lippiatt et al., 2010; Brown et al., 2012).

Table 1
Surface water data. (1a) Sampling location and water properties: salinity, temperature (ship's data), nutrient and oxygen concentrations (from WOA '05; see text). (1b) Nd isotope compositions, REE concentrations, Ce-anomaly, heavy-to-light REE ratio, middle-REE enrichment and weightings from the multivariate analyses (see text). Errors, in italics, represent 2σ external reproducibilities of Nd isotope compositions (this study) and REE concentration data (given as percent error (2σ); for further details see Hathorne et al., 2012).

Panel 1a

Sample ID	Date sampled	Sample type	Bottom water depth (m)	Lat. (degrees)	Lat. (minutes)	Lon. (degrees)	Lon. (minutes)	Salinity (PSU)	Temp. (°C)	Nitrate & nitrite (μM)	Phosphate (μM)	Silicic acid (μM)	Oxygen (ml/l)
1	8/19/07	Fish	130.6	59	3.2	138	45.0	28.36	12.91	7.30	1.03	17.70	6.67
2	8/19/07	Fish	190.0	59	23.5	140	8.8	28.63	15.81	6.40	1.13	15.80	6.76
3	8/20/07	Fish	54.0	59	41.4	141	14.9	28.89	10.88	7.90	1.27	17.50	6.87
4	8/20/07	Fish	57.0	59	53.3	142	4.3	23.37	10.67	7.90	1.27	17.50	6.87
5	8/24/07	Fish	3866.0	56	10.7	143	51.9	32.05	13.89	10.10	1.24	19.40	6.81
13	8/25/07	CTD 018-1	3654.0	56	60.0	142	30.0	31.79	14.20	9.70	1.22	19.30	6.79
21	8/26/07	CTD 023-3	3594.0	58	43.0	144	0.0	32.52	13.45	8.30	1.21	16.90	6.84
22	8/27/07	Fish	44.0	60	8.0	144	45.5	27.78	14.01	7.80	1.16	15.60	6.85
23	8/27/07	Fish	46.0	60	11.1	145	22.9	24.60	14.01	7.70	1.10	15.10	6.86
24	8/27/07	Fish	32.4	60	18.6	146	0.8	21.34	14.32	7.80	1.06	14.70	6.90
26	8/30/07	Fish	213.0	59	37.5	149	15.4	30.38	13.21	8.10	0.96	14.80	7.02
27	8/30/07	Fish	170.0	59	15.9	148	54.6	32.13	13.06	8.10	0.96	14.80	7.02
28	8/30/07	Fish	284.0	58	41.4	148	20.7	32.42	13.78	8.10	1.01	14.60	7.02
29	8/30/07	Fish	2128.0	58	8.9	147	51.4	32.52	13.22	8.50	1.07	15.50	6.95
33	9/1/07	CTD 033-1	185.0	58	54.0	152	49.0	31.29	11.01	5.90	0.95	11.60	7.28
41	9/10/07	CTD 054-2	5000.0	54	20.0	155	33.1	32.44	12.25	11.00	1.27	24.70	7.03
42	9/14/07	Fish	4987.0	54	39.6	158	2.2	32.55	11.78	11.80	1.32	25.80	7.01
44	9/16/07	Fish	4688.0	54	7.4	155	0.7	32.26	12.07	11.10	1.27	24.70	7.03
45	9/16/07	Fish	3786.0	54	56.1	155	5.6	32.12	10.73	11.50	1.29	24.60	7.00
46	9/17/07	Fish	112.0	56	5.2	154	40.1	31.75	10.83	10.70	1.24	22.50	7.05
25	8/27/07	Hand: Copper River	5.0	60	24.8	145	40.8	0.00	0.00	n/a	n/a	n/a	n/a

(*continued on next page*)

Table 1. (*continued*)

Panel 1b

Sample ID	εNd	La (pM)	Ce (pM)	Pr(pM)	Nd (pM)	Sm (pM)	Eu (pM)	Gd (pM)	Tb (pM)	Dy (pM)	Ho (pM)	Er (pM)	Tm (pM)	Yb (pM)	Lu (pM)	Ce/Ce*	HREE/LREE	MREE*	OR1: with Ce		OR2: without Ce	
Error	*0.35*	*6.2*	*14.8*	*11.5*	*9.5*	*22.2*	*15.1*	*15.5*	*14.3*	*10.7*	*10.0*	*9.3*	*12.3*	*11.6*	*8.0*				F1	F2	F1	F2
1	−0.52	14.78	19.37	2.92	11.69	2.50	0.90	3.82	0.65	4.55	1.19	3.64	0.65	3.99	0.73	0.68	4.56	1.01	0.0	1.0	0.7	0.3
2	−0.73	20.74	16.14	3.60	15.98	3.15	1.02	4.48	0.79	5.48	1.29	4.32	0.61	3.91	0.68	0.42	3.34	1.19	0.2	0.8	0.4	0.6
3	−0.64	20.94	13.96	3.35	15.85	3.84	1.05	4.85	0.76	5.60	1.37	4.90	0.75	4.63	0.84	0.38	4.21	1.03	0.4	0.7	0.6	0.4
4	−0.19	34.80	26.15	5.89	25.29	5.73	2.43	9.91	1.67	13.28	3.65	12.42	1.93	12.63	2.26	0.41	6.83	0.94	0.5	0.5	1.0	0.0
5	−2.31	12.27	3.57	1.68	7.38	0.81	0.33	1.95	0.28	2.27	0.63	2.18	0.34	1.69	0.27	0.17	2.98	1.09	0.6	0.4	0.3	0.8
13	−1.02	17.41	5.72	2.58	12.00	2.63	0.65	3.41	0.48	3.94	1.04	3.32	0.50	2.77	0.46	0.19	3.15	1.14	0.6	0.4	0.3	0.7
21	−2.04	12.79	2.86	1.42	6.74	1.44	0.38	1.96	0.24	2.04	0.62	2.67	0.35	1.54	0.24	0.14	3.02	1.07	0.7	0.3	0.2	0.8
22	0.07	n/a	n/a	n/a	n/a	n/a	n/a	n/a	n/a	n/a	n/a	n/a	n/a	n/a	n/a	n/a	n/a	n/a	n/a	n/a	n/a	n/a
23	0.05	39.93	36.59	6.69	29.22	5.74	2.25	9.42	1.37	11.61	2.90	9.81	1.48	9.73	1.81	0.51	4.68	0.96	0.2	0.8	0.7	0.3
24	0.21	22.13	15.28	3.52	15.19	5.45	1.19	4.82	0.81	6.34	1.96	6.41	1.07	6.78	1.18	0.39	6.02	0.84	0.5	0.6	0.9	0.1
26	−0.50	20.60	11.24	3.64	14.50	3.18	0.95	4.65	0.75	5.80	1.44	4.60	0.68	3.87	0.69	0.30	3.52	1.21	0.5	0.6	0.4	0.6
27	−1.32	12.78	5.11	2.04	9.10	1.22	0.54	2.67	0.41	3.02	0.88	2.67	0.43	2.01	0.34	0.23	2.99	1.23	0.6	0.5	0.3	0.7
28	−2.14	12.08	4.18	1.64	7.44	1.24	0.33	1.75	0.31	2.80	0.68	2.26	0.34	1.60	0.24	0.21	2.78	1.36	0.6	0.5	0.2	0.8
29	−1.92	13.45	4.20	1.71	7.18	1.25	0.38	2.47	0.29	2.66	0.78	2.43	0.36	2.01	0.23	0.19	3.07	1.20	0.6	0.5	0.2	0.8
33	−0.55	18.00	8.40	3.02	12.96	2.70	0.96	3.89	0.72	5.01	1.26	4.17	0.58	3.62	0.65	0.26	3.83	1.19	0.6	0.5	0.5	0.5
41	−2.03	15.89	3.68	2.10	9.26	2.48	0.48	3.28	0.45	3.39	0.91	2.94	0.43	2.30	0.39	0.14	3.33	1.23	0.7	0.3	0.3	0.7
42	−2.06	16.32	3.37	2.29	9.92	1.80	0.56	2.65	0.41	3.31	0.95	3.08	0.42	2.35	0.37	0.12	3.06	1.15	0.8	0.3	0.3	0.7
44	−1.86	14.52	9.34	1.79	7.99	0.88	0.33	2.35	0.26	2.59	0.63	2.40	0.27	1.70	0.22	0.40	2.51	1.21	0.0	1.0	0.0	1.0
45	−0.85	15.74	7.04	2.20	9.74	1.18	0.59	3.46	0.42	3.52	0.90	3.46	0.42	2.89	0.42	0.27	3.72	1.07	0.5	0.6	0.4	0.6
46	−0.52	16.80	15.70	2.57	13.41	1.51	0.82	3.76	0.59	4.13	1.14	3.81	0.56	3.47	0.56	0.54	3.65	1.07	0.1	0.9	0.4	0.6
25	−3.75	136.21	230.45	30.40	125.13	24.98	6.89	29.95	4.64	27.76	6.07	17.39	2.51	14.98	2.40	0.99	1.44	1.39	n/a	n/a	n/a	n/a

Table 2
Profile data. (2a) Sampling position and water properties: salinity, temperature (ship's data) and nutrients and oxygen (from WOA '05; see text). (2b) Nd isotope, REE concentration, Ce-anomaly, heavy-to-light REE ratio, middle-REE enrichment and weightings from the multivariate analyses (see text). Errors, in italics, represent 2σ external reproducibilities of Nd isotope compositions (this study) and REE concentration data (given as percent error (2σ); for further details see Hathorne et al., 2012).

Panel 2a

Sample ID	Date sampled	Sample type	Bottom water depth (m)	Lat. (degrees)	Lat. (minutes)	Lon. (degrees)	Lon. (minutes)	Sample depth (m)	Salinity (PSU)	Temp. (°C)	Nitrate &nitrite (μM)	Phosphate (μM)	Silicic acid (μM)	Oxygen (ml/l)
6	8/25/07	CTD 018-1	3654	56	60.0	142	30.0	3500.00	34.68	1.46	37.10	2.63	176.40	3.01
7	8/25/07							2500.00	34.64	1.69	42.10	2.87	184.00	2.04
8	8/25/07							1500.00	34.51	2.32	45.10	3.15	167.10	0.77
9	8/25/07							900.00	34.30	3.43	42.50	3.22	129.10	0.49
10	8/25/07							400.00	34.03	4.42	40.10	3.06	88.40	0.97
11	8/25/07							250.00	33.84	4.99	32.90	2.84	60.50	1.70
12	8/25/07							100.00	32.60	5.64	21.00	1.88	34.60	5.56
13	8/25/07							10.00	31.79	14.20	9.10	1.19	18.80	6.82
14	8/26/07	CTD 023-3	3594	58	43.0	144	0.0	3500.00	34.69	1.42	35.50	2.56	175.50	2.94
15	8/26/07							2500.00	34.64	1.69	34.64	2.82	189.30	2.06
16	8/26/07							1500.00	34.53	2.23	46.20	2.92	168.60	0.80
17	8/26/07							900.00	34.36	3.04	39.70	3.24	118.90	0.45
18	8/26/07							400.00	34.09	4.00	39.40	2.98	88.90	1.06
19	8/26/07							250.00	33.94	4.28	29.10	2.77	51.80	2.00
20	8/26/07							100.00	33.04	3.90	18.30	1.84	29.70	5.82
21	8/26/07							10.00	32.52	13.45	8.50	1.21	16.30	6.85
30	9/1/07	CTD 033-1	185	58	54.0	152	49.0	175.00	32.50	4.65	31.60	2.26	49.90	4.34
31	9/1/07							125.00	32.27	6.37	25.00	1.51	27.60	6.11
32	9/1/07							75.00	32.02	7.46	14.00	1.39	21.40	6.54
33	9/1/07							10.00	31.29	11.01	6.80	0.99	13.00	7.22
34	9/10/07	CTD 054-2	5000	54	20.0	155	33.1	5000.00	34.69	1.54	36.50	2.54	154.30	3.63
35	9/10/07							3000.00	34.66	1.55	39.10	2.74	172.60	2.66
36	9/10/07							2000.00	34.60	1.85	42.20	3.03	176.30	1.57
37	9/10/07							1000.00	34.40	2.84	44.80	3.21	150.00	0.49
38	9/10/07							750.00	34.30	3.25	44.80	3.20	137.95	0.48
39	9/10/07							300.00	34.02	4.03	44.80	3.04	95.70	1.17
40	9/10/07							100.00	33.24	3.62	25.30	2.04	44.80	5.20
41	9/10/07							10.00	32.44	12.25	12.20	1.27	25.90	7.04

(*continued on next page*)

Table 2. (*continued*)

Panel 2b

Sample ID	εNd	La (pM)	Ce (pM)	Pr (pM)	Nd (pM)	Sm (pM)	Eu (pM)	Gd (pM)	Tb (pM)	Dy (pM)	Ho (pM)	Er (pM)	Tm (pM)	Yb (pM)	Lu (pM)	εNd	HREE/ LREE	MREE*	OR1: with Ce		OR2: without Ce	
	0.35	*6.2*	*14.8*	*11.5*	*9.5*	*22.2*	*15.1*	*15.5*	*14.3*	*10.7*	*10.0*	*9.3*	*12.3*	*11.6*	*8.0*	*0.35*			F1	F2	F1	F2
6	−3.13	66.02	3.82	10.13	43.38	8.88	2.50	12.67	2.07	13.98	3.82	12.95	1.99	14.08	2.44	0.03	4.36	0.91	1.0	0.0	0.6	0.4
7	−2.70	53.36	6.07	7.04	32.39	5.45	1.65	9.62	1.58	12.26	3.35	10.46	1.77	13.69	2.33	0.07	5.81	0.81	1.0	0.0	0.9	0.1
8	−2.56	44.81	4.38	5.60	23.38	4.50	1.38	6.96	1.13	10.00	2.71	9.16	1.41	10.60	1.81	0.06	5.97	0.81	1.0	0.0	0.9	0.1
9	−2.51	n/a	n/a	n/a	n/a	n/a	n/a	n/a	n/a	n/a	n/a	n/a	n/a	n/a	n/a	n/a	n/a	n/a	n/a	n/a	n/a	n/a
10	−2.78	n/a	n/a	n/a	n/a	n/a	n/a	n/a	n/a	n/a	n/a	n/a	n/a	n/a	n/a	n/a	n/a	n/a	n/a	n/a	n/a	n/a
11	−2.83	n/a	n/a	n/a	n/a	n/a	n/a	n/a	n/a	n/a	n/a	n/a	n/a	n/a	n/a	n/a	n/a	n/a	n/a	n/a	n/a	n/a
12	−1.54	19.77	5.55	2.93	12.45	2.13	0.67	3.45	0.63	4.50	1.15	4.11	0.56	3.38	0.64	0.16	3.81	1.10	0.7	0.3	0.5	0.5
13	−1.02	17.41	5.72	2.58	12.00	2.63	0.65	3.41	0.48	3.94	1.04	3.32	0.50	2.77	0.46	0.19	3.15	1.14	0.6	0.4	0.3	0.7
14	−3.41	66.16	3.92	9.95	45.92	9.99	2.54	12.32	2.00	14.41	3.75	12.37	1.94	13.63	2.36	0.03	4.12	0.93	1.0	0.0	0.6	0.4
15	−2.12	54.90	4.53	7.42	32.95	6.59	1.48	9.70	1.61	12.84	3.62	11.97	1.69	13.35	2.45	0.05	5.69	0.83	1.0	0.0	0.9	0.1
16	−2.51	49.99	6.66	5.92	29.03	6.31	1.64	8.32	1.20	9.64	2.66	9.82	1.56	10.80	2.01	0.08	5.50	0.76	0.9	0.1	0.9	0.1
17	−2.56	38.62	4.38	4.75	22.28	3.58	1.12	6.42	0.88	7.84	2.18	7.68	1.32	7.71	1.45	0.07	5.05	0.81	0.9	0.1	0.8	0.2
18	−2.75	36.97	6.09	4.66	21.71	3.14	1.02	7.36	0.78	7.32	2.11	6.45	0.94	6.50	1.22	0.10	4.34	0.86	0.8	0.2	0.6	0.5
19	−2.51	n/a	n/a	n/a	n/a	n/a	n/a	n/a	n/a	n/a	n/a	n/a	n/a	n/a	n/a	n/a	n/a	n/a	n/a	n/a	n/a	n/a
20	−2.66	23.37	4.49	3.01	13.51	2.96	0.63	4.06	0.60	4.60	1.17	4.12	0.62	3.98	0.66	0.12	3.95	1.00	0.8	0.2	0.5	0.5
21	−2.04	12.79	2.86	1.42	6.74	1.44	0.38	1.96	0.24	2.04	0.62	2.67	0.35	1.54	0.24	0.14	3.02	1.07	0.7	0.3	0.2	0.8
30	−0.19	17.86	8.55	2.86	10.80	2.28	0.73	3.78	0.61	5.25	1.24	4.19	0.64	4.33	0.69	0.27	4.86	1.06	0.6	0.5	0.7	0.3
31	−0.79	17.88	4.11	2.83	11.01	2.97	0.70	3.80	0.72	4.65	1.28	4.15	0.61	3.53	0.64	0.13	4.23	1.19	0.8	0.2	0.6	0.4
32	−0.42	18.13	4.28	3.04	13.50	2.81	0.69	4.28	0.64	5.01	1.26	4.09	0.65	4.07	0.57	0.13	3.72	1.13	0.8	0.2	0.5	0.5
33	−0.55	18.00	8.40	3.02	12.96	2.70	0.96	3.89	0.72	5.01	1.26	4.17	0.58	3.62	0.65	0.26	3.83	1.19	0.6	0.5	0.5	0.5
34	−3.49	63.60	7.40	9.89	42.53	8.59	2.39	11.96	2.10	14.43	3.45	11.51	1.78	12.20	2.16	0.07	3.90	1.04	0.9	0.1	0.5	0.5
35	−3.09	54.67	11.82	7.58	32.19	7.00	1.76	9.04	1.67	12.42	3.12	10.72	1.68	12.61	2.11	0.13	5.14	0.90	0.8	0.2	0.8	0.2
36	−2.32	49.92	6.21	6.18	27.17	4.67	1.38	8.83	1.38	10.92	3.11	9.91	1.54	12.40	2.20	0.08	6.27	0.79	0.9	0.1	1.0	0.0
37	−2.44	40.91	6.56	5.00	21.77	3.95	1.25	6.76	1.10	8.66	2.30	8.12	1.29	8.93	1.55	0.10	5.55	0.86	0.9	0.1	0.8	0.2
38	−2.27	37.53	4.40	4.55	20.60	3.93	0.99	5.52	0.98	8.14	2.13	6.96	1.17	7.83	1.30	0.07	5.11	0.91	0.9	0.1	0.8	0.2
39	n/a	34.64	4.03	4.36	18.22	3.19	1.06	4.76	0.97	6.45	1.90	5.75	0.92	6.42	1.03	0.07	4.50	0.97	0.9	0.1	0.6	0.4
40	−2.15	24.51	4.16	3.23	14.03	2.48	0.64	4.47	0.66	5.21	1.26	4.36	0.72	3.90	0.64	0.10	3.66	1.13	0.8	0.2	0.4	0.6
41	−2.03	15.89	3.68	2.10	9.26	2.48	0.48	3.28	0.45	3.39	0.91	2.94	0.43	2.30	0.39	0.14	3.33	1.23	0.7	0.3	0.3	0.7

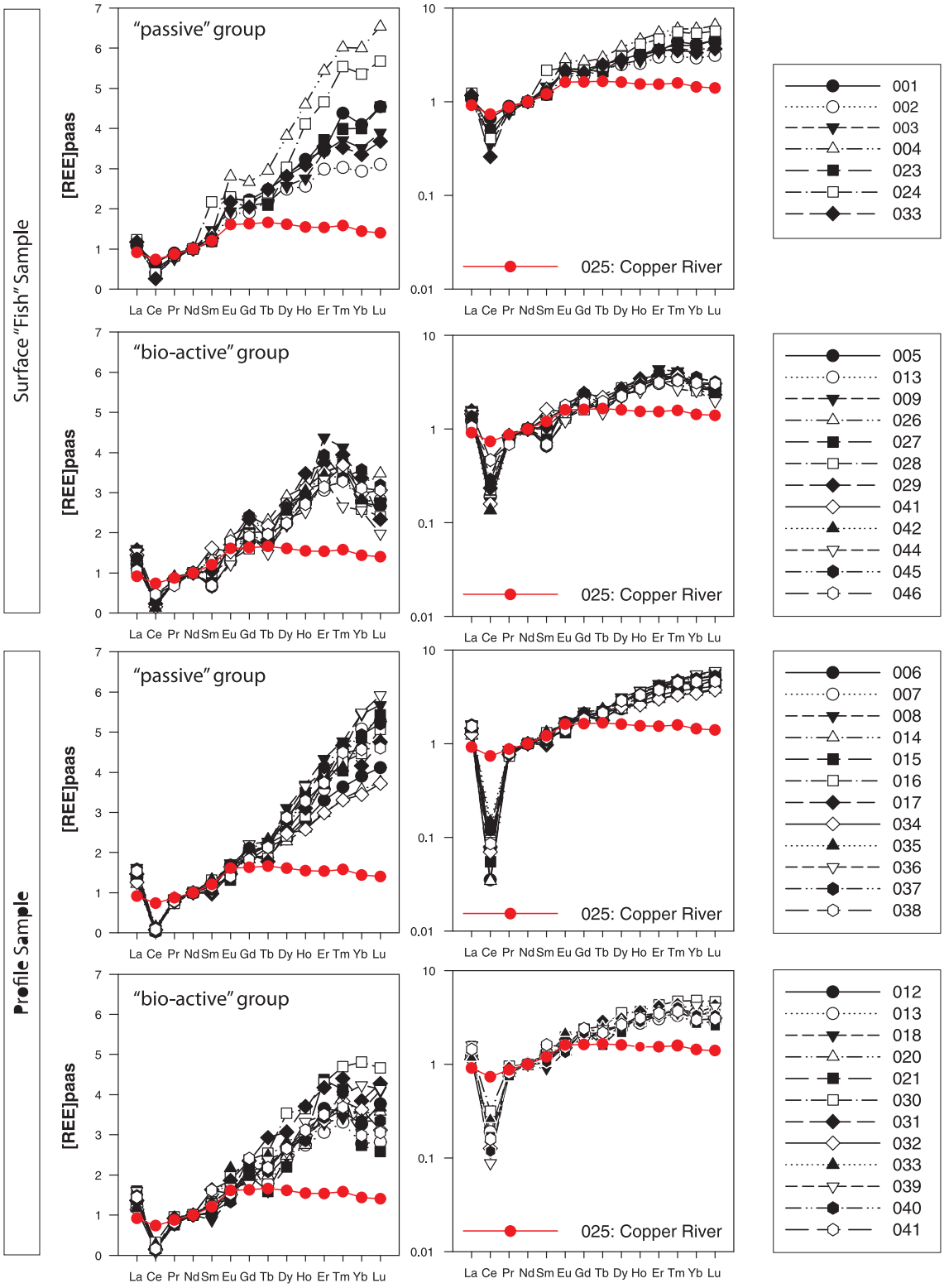

Fig. 4. REE patterns. All data are normalized to PAAS (Nance and Taylor, 1976) and Nd concentrations, in order to be able to better compare patterns (Note: data are presented on both linear (left) and log (right) scales). *Upper panels*: Surface sample "passive" and "bio-active" groups; *Lower panels*: Depth profiles of the "passive" and "bio-active" groups. The Copper river sample is given in red for comparison.

3.1.2. REEs

In general, two distinct types of surface samples were analyzed: One set of samples from the eastern-most Alaskan coast referred to as the "passive" group (samples 001–004, 023, 024 and 033), and a set of samples from the central gyre region and southern/southwestern coast of

Alaska referred to as the "bio-reactive" group (samples 005; 013; 021; 026–029; 041; 042; 044–046). (This nomenclature will be explained further in the discussion section.) The "passive" samples have a mean [La] of 25 pM, within a large range between ~15 and 40 pM, compared to the "bio-reactive" samples with a mean [La] of ~15 pM and a smaller range of ~12–20 pM (Table 1). The higher mean and larger range of [La] in the "passive" samples holds for all other REEs as well and is generally more pronounced for the HREEs. For example, where Nd is ~2 times more concentrated on average and has a ~225% larger range in the "passive" versus "bio-reactive" samples, Lu is on average 3.2 times more concentrated with a >300% greater range in the "passive" versus "bio-reactive" samples. Cerium (Ce), which undergoes microbially-mediated redox chemistry in the oceans (Moffett, 1990, 1994), has a higher (>3 times greater) average in "passive" samples over "bio-reactive" samples (Table 1). More complete statistical analyses distinguishing the two groups are presented below.

The REE concentration patterns are compared through *both* a shale normalization (PAAS; Nance and Taylor, 1976) *and* normalization to the measured Nd concentration of each given sample in Fig. 4. This double normalization better illustrates the REE patterns, and supports our arbitrary groupings, given that the distinction between "passive" and "bio-reactive" samples is clear in these patterns. "Bio-reactive" samples are more tightly clustered and are accompanied by a distinct reduction in the HREE abundances, as compared to the more variable and linearly increasing HREE abundances observed for the "passive" patterns. The pattern of the Copper River estuary (CRE) sample (025) is shown in each plot for comparison,

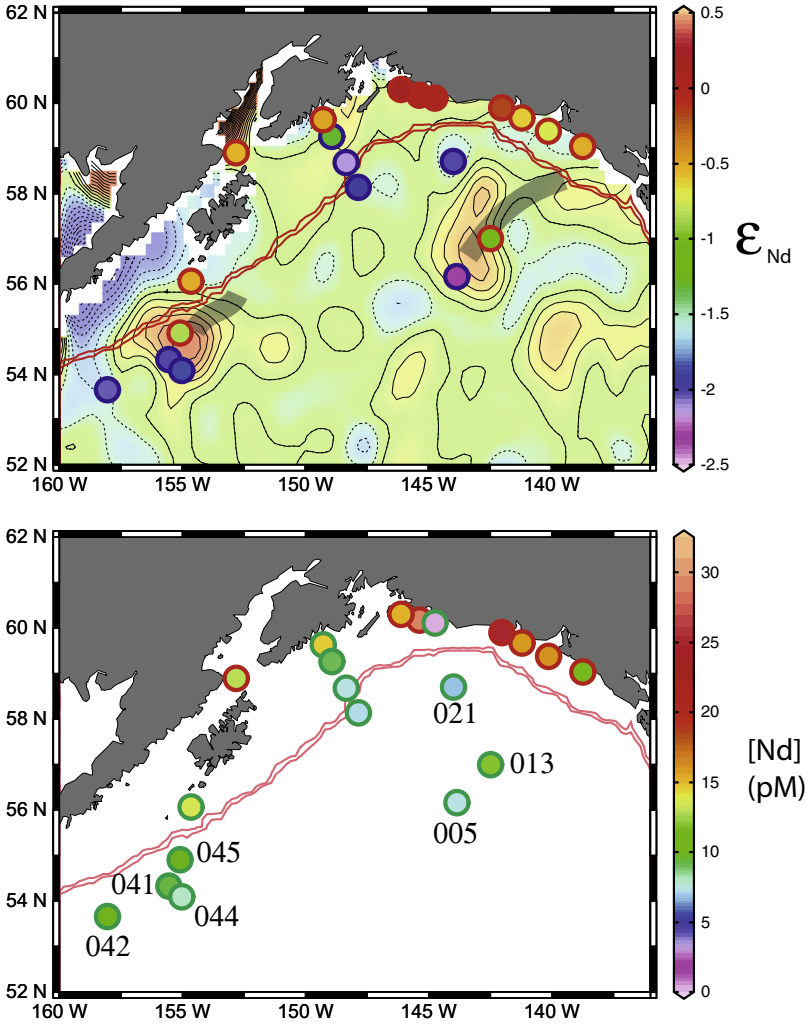

Fig. 5. Surface sample εNd (upper panel) and Nd concentrations (lower panel). Data points circled in red in the upper panel indicate εNd > −1 while blue circles indicate εNd < −1. Nd concentration data points circled in red (lower panel) indicate samples with a "passive" REE pattern and the green ones indicate samples with a "bio-active" REE pattern (see text for details). Also shown are the sea surface height anomalies (from CCAR, University of Colorado). The shelf break is delimited by the double red-bathymetric lines. Sample numbers in the lower panel are given for samples near or in the sampled eddies. The gray arrows indicate the general migration path of the eddies, but during the sampling period the eddies were both stalled and generally dissipating. (For interpretation of the references to color in this figure legend, the reader is referred to the web version of this article.)

although this sample did not have zero salinity and thus may not represent a true REE riverine end-member (Sholkovitz, 1992, 1993; Sholkovitz and Szymczak, 2000). However, the flattened-pattern with only slight MREE enrichment and weakly developed Ce anomaly (i.e., general similarity to shale) is typical for rivers (Elderfield et al., 1990). Rare earth element patterns are conventionally characterized and discussed on the basis of some simplified parameters: the Ce-anomaly, the "slope" (HREE/LREE) and the concavity or convexity (MREE/MREE*; Table 1). The "passive" samples have, on average, larger Ce/Ce* (0.4 versus 0.2 for "bio-reactive" samples) and steeper slopes

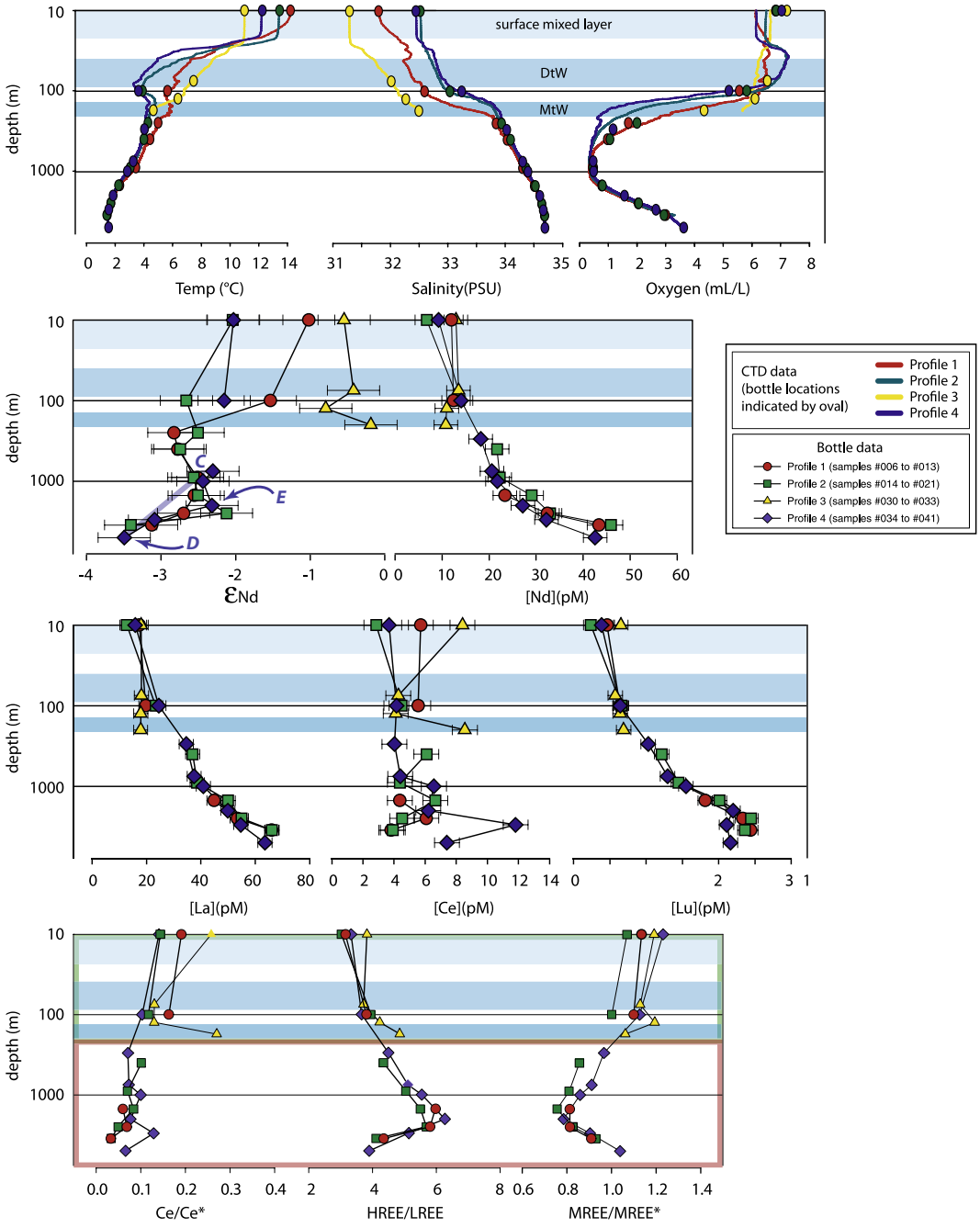

Fig. 6. Depth profile data. *Upper panel*: Temperature, salinity, and oxygen. *Upper middle panel:* εNd and Nd concentration (pM); *Lower middle panel*: Lanthanum, cerium and lutetium concentrations (pM); *Bottom panel*: Ce-anomaly; HREE/LREE and MREE-anomaly. Here defining $Ce/Ce^* = [Ce]_N/\text{average}([La]_N;[Pr]_N))$; $HREE/LREE = ([Yb]_N + [Lu]_N)/([Pr]_N + [Nd]_N)$; $MREE/MREE^* = ([Tb]_N + [Dy]_N)/(\text{average of } [Pr]_N,[Nd]_N,[Yb]_N \text{ and } [Lu]_N)$; where "N" refers to PAAS-normalized REEs. Note the logarithmic vertical (depth) scales. The annotations "C", "D", and "E", and the blue line in the εNd figure illustrate the differences described in the text. The samples described here as "bio-active" all represent near surface waters shown by the green box in the bottom panel. The "passive" samples in the orange box in the bottom panel are from deeper waters.

(HREE averages 4.8 in "passive" samples versus 3.1 in "bio-reactive" samples). Both groups display similar MREE/MREE* (1.0 and 1.2 for "passive" and "bio-reactive", respectively; Table 1).

3.1.3. Nd isotopes

Surface water Nd isotope signatures range from −2.3 to +0.6, whereby the most positive εNd values are generally found closer to the coast (Fig. 5). It is also apparent from Fig. 5 that the Nd isotopes are generally more radiogenic inshore of the shelf break, and less radiogenic for the offshore open waters. The two samples collected near the core of the two eddies (013 and 045) are distinctly more radiogenic than the samples outside the eddy (005, 021, 041, 042 and 044; Fig. 5). The locations of these samples may not exactly coincide with the cores of the eddies (Fig. 5) given that for the date of sampling the precise locations of the eddy differed somewhat. However, the most radiogenic samples clearly represent waters in or near the core of the eddy, making these data consistent with formation of near-shore eddies transporting waters from the coast to the central gyre of the GoA (Ladd et al., 2005, 2009).

3.2. Subsurface waters

3.2.1. Hydrographic properties

Similar to the surface waters, the temperature, salinity, nutrient ("nitrate", phosphate, silicate) and oxygen data of the depth profiles correlate well with the WOA '05 annual estimates from nearby locations, except at surface and mixed layer depths where seasonal differences between these data sets are seen. The good correspondence between the data sets allow the use of the more complete WOA '05 database for comparison of the hydrography to the REE and Nd isotope data (Table 2).

3.2.2. REEs

The REE profiles are consistent with previously measured open ocean profiles in that they all show increasing REE concentrations, particularly the HREEs, with water depth (Table 2; Fig. 6). The concentrations of each REE at a given depth are similar at all three deep stations. Again, due to its different redox-dependent behavior, Ce shows anomalously low concentrations and roughly constant concentrations with water depth (Fig. 6).

The REE patterns for depths greater than 400 m are of the "passive" type; that is, the deep-water samples all show a linearly increasing trend towards heavier REEs (normalized to PAAS and Nd as described above) and a clear Ce-anomaly (Fig. 4). The samples taken from 400 m or shallower resemble the "bio-reactive" type. Fig. 6 displays the variations of Ce/Ce*, MREE/MREE* and HREE/LREE of these samples with water depth: Ce/Ce* decreases consistently with depth (by ~0.1unit or >70%); MREE/MREE* decreases from a surface value of ~1.1 to ~0.8 between 1500 and 2000 m depth, then increases again towards ~1.0 at bottom depths; HREE/LREE increases from ~3 at the surface to >6 at depths between 1500 and 2000 m depth and then decreases again towards the bottom of the profiles (Fig. 6).

3.2.3. Nd isotopes

All Nd isotope profiles are identical within error at depths below the seasonally mixed layer (i.e., MtW). The deep waters are more radiogenic in εNd, at ~−3 to ~−2.5 between 750 and 2000 m depth, and then decrease to −3.5 in the abyssal ocean (Fig. 6). The more radiogenic signature of the coastal waters is most pronounced in the depth profile of CTD033 taken in the Cook Inlet (Fig. 3).

While surface waters sampled in the cores of the eddies are more radiogenic (−1 to −1.5), consistent with these waters originating from a near-coastal source, the waters immediately below the eddy-influenced mixed layers (i.e., below MtW; Ladd et al., 2009) are similar for all profiles (Fig. 6; Table 2). These observations suggest that the eddies of the Gulf of Alaska efficiently transport dissolved metals from the shelf to the central gyre region and that slope-derived metals below the mixed layer are not influenced by the eddies: if the REEs are considered representative. This is an inference that has implications for the distribution and potential supply pathways of metals acting as micronutrients such as Fe (Ladd et al., 2009; Lippiatt et al., 2010).

4. DISCUSSION

4.1. Nd isotope distribution in the Gulf of Alaska

Fig. 7 shows the three deep-water column profiles in temperature–salinity–Nd isotope parameter space (T/S/εNd). If Nd isotopes indeed act as conservative tracers of water mass mixing, the εNd data should not significantly deviate from the T/S curves that delimit water masses (large grey dots) and the mixing lines connecting them, given that

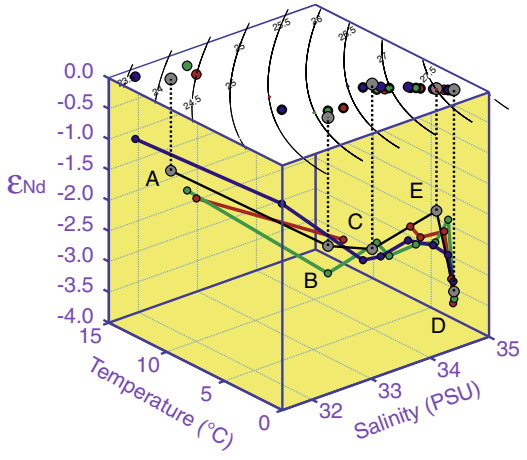

Fig. 7. Temperature (*y*-axis), salinity (*x*-axis) and εNd (*z*-axis) profile data. (A) Surface water; (B) Dicothermal Water; (C) mesothermal water; (D) Pacific Deep Water. Colored circles represent bottle samples taken for REE and Nd isotopes; Grey circles represent modeled mixing "end-members." The εNd signature of point E is not discernable through temperature or salinity characteristics, but has a distinct (by ~1 unit) εNd (see text for discussion). (For interpretation of the references to color in this figure legend, the reader is referred to the web version of this article.)

Table 3
GoA water mass characteristics. Temperature, salinity and Nd isotopic fingerprint for mid-depths of water masses in the GoA, as inferred from the data collected during this cruise, and from Talley et al. (2011). The HREE/LREE and MREE/MREE* are also listed for these water masses.

	Water mass	Temperature (°C)	Salinity (PSU)	εNd	[Nd]/ (pM)	HREE/ LREE	MREE/ MREE*	Approx. depth (m)
A	Surface	10.7–14.2 (12.7)	30.4–32.6 (32.1)	−0.5 to −2.3 (−1.5)	10	3	1.2	Mixed layer
B	Dicothermal water	3.2	32.9	−2.110	10	3.5	1.2	100
C	Mesothermal water	5.0	34.0	−2.7	20	5	0.9	750–1000
D	PDW	1.1–1.2	34.7	−3.5	45	4	1.0	3500+
E	Unknown	2.3	34.5	−2.2	30	6	0.7	2000–2500

the [Nd] differences between the end-member water masses are small. There are four main inflections in the T/S data that approach "pure" water mass end-members, all of which are marked by distinct εNd signatures and are thus consistent with conservative behavior. These four water masses are identified as the surface mixed layer (A), the dichothermal layer (DtW; B), the mesothermal layer (MtW; C), and Pacific Deep Water (PDW; D) (Talley, 2007). There is, however, one significant deviation towards more radiogenic signatures by ~1 εNd units in the deep waters where there is none expected from T/S space (point E in Fig. 7; also shown in the εNd plot in Fig. 6), and which cannot be reached by mixing given that *both* possible end-members are less radiogenic (i.e., points C and D versus E). This raises the question of whether εNd always behaves "conservatively", when there are deviations even at mid-depths at a significant distance from ocean margins.

To address this question, our initial hypothesis is that PDW can be divided into waters of different origin that are not apparent in T/S space alone. The inflection point E estimated in Fig. 7 is defined by 2.3 °C, 34.6 PSU and −2.0 εNd, which corresponds (in T/S space) to a water mass centered at 2200 m depth (Table 3). This is consistent with ^{14}C data, which follow a similar pattern and indicate that the oldest waters in the deep Pacific are found near 2000 m depth in the North Pacific region (Talley, 2007). In fact, the age estimate of this mid-abyssal water mass (~1000 years; Talley, 2007) is similar to or greater than the estimates of the global average deep water residence time of Nd (e.g., Arsouze et al., 2009; Rempfer et al., 2011), implying that this εNd signature may not only reflect contemporaneous mixing processes. That is, the εNd signature of this mid-depth water mass is significantly more positive (−2 εNd) than our observations of modern PDW (at -3.5 εNd or lower), modern NPIW, or shallower waters (all <−2.5 εNd), which implies that this mid-depth water mass may be retaining an older εNd signature of the deep North Pacific that has not yet been lost through diffusion and mixing. Furthermore, if this water mass indeed represents an isolated snapshot of past PDW, this may suggest that this εNd signature reflects a past state, during which the north Pacific was less influenced by southern deep-water sources (which generally are characterized by significantly more negative εNd signatures). That is, the "modern" deep Pacific circulation pattern, as seen by εNd, include and integrate changes that occurred over the past thousand years.

A second possible hypothesis is that it is not the mid-depth, but rather the bottom water εNd that diverges in T/S/εNd parameter space (Fig. 7). Bottom waters may be influenced by interactions with the sediments, possibly via pore water inputs (Haley et al., 2004) or boundary exchange (Lacan and Jeandel, 2001, 2005; Carter et al., 2012; Singh et al., 2012; Stichel et al., 2012a,b). In either case, but particularly the latter, there are implications for the "quasi conservative" nature of εNd in the deep ocean. A mixing diagram defined by Nd isotope compositions and concentrations (Fig. 8) offers some insight into this issue, given that straight lines in these plots indicate conservative mixing between two end-members. Piepgras and Jacobsen (1988) used such a diagram to infer Nd removal in bottom waters (black line in Fig. 8). Our few bottom water samples (filled blue circles; Fig. 8) are consistent with the data of Piepgras and Jacobsen (1988). Such a *loss* of Nd, as also observed elsewhere (e.g., Piepgras and Jacobsen, 1988; Grasse et al., 2012), should not be accompanied by shifts in Nd isotopic compositions of the bottom waters, unless complex exchange processes with the deep sea sediments are invoked; such a loss term would also contradict a simple pore water Nd source function (Haley and Klinkhammer, 2003; Haley et al., 2004), as will be discussed later. In view of these arguments and despite the general consistency of the GoA bottom water εNd (solid blue circles; Fig. 8) with those of Piepgras and Jacobsen (1988; solid black squares and black line), we consider the possibility of a bottom water εNd divergence in T/S/εNd parameter space that is caused by Nd loss to be less likely than the first hypothesis presented above. Further discussion on the possibility for a REE loss term during interaction with sediments is given in Section 4.2.

A third possible hypothesis to explain the T/S/εNd data is that the mid-depth εNd is affected by exchange with the shelf and slope (Lacan and Jeandel, 2005). Plumes of geochemically altered water off the shelf are known to affect Fe concentrations in mid-depth waters (Laes et al., 2003), as well as Nd and Hf isotopes and concentrations (Rickli et al., 2010; Grasse et al., 2012; Singh et al., 2012). In a moderate-sized and semi-enclosed basin such as the Gulf of Alaska, shelf/slope processes may have significant

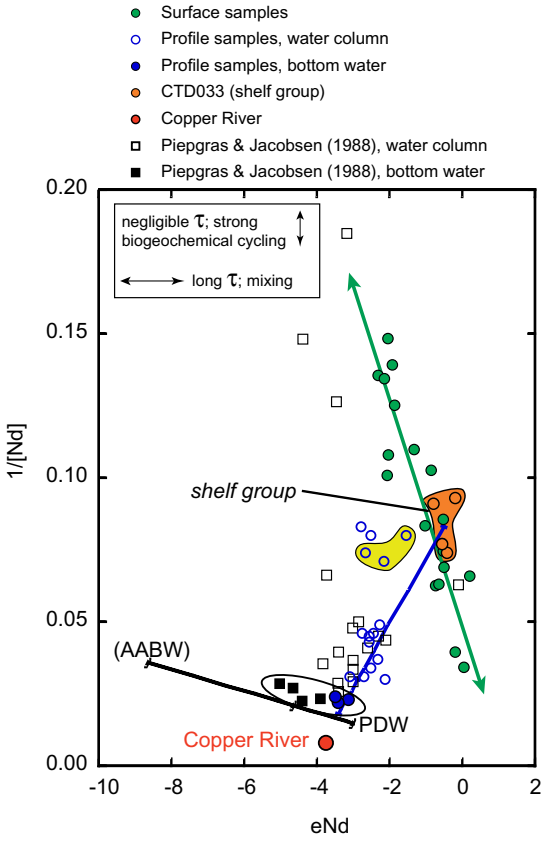

Fig. 8. Nd-isotope mixing plot. The black mixing line between PDW (Pacific Deep Water) and AABW (Antarctic Bottom Water) represents bottom water samples from Piepgras and Jacobsen (1988) (black squares). Note that no AABW was measured in this work. The blue line describes theoretical mixing of shelf/subsurface and abyssal waters (i.e., PDW). The green mixing line implies that the surface samples can all be explained by two-component mixing with a strong biogeochemical cycling. The three samples in yellow are from 100 m depth taken "in the wake" of an eddy. (For interpretation of the references to color in this figure legend, the reader is referred to the web version of this article.)

transient impacts on mid-depth dissolved metal characteristics. As with the preceding hypothesis, we can use the mixing diagram (Fig. 8) to investigate this idea. There is clearly a possible mixing line that encompasses the deep, mid-depth and shelf water data of this study as well as those of Piepgras and Jacobsen (1988) (blue line in Fig. 8). This line can be generated through mixing of shelf waters ("shelf group"; Fig. 8) with a source that approaches the PDW end-member inferred by Piepgras and Jacobsen (1988). The possibility for such a mixing trend between shelf and abyssal water is important for our understanding of the factors controlling the distribution of oceanic εNd signatures, particularly regarding the mechanisms by which the deep Pacific Ocean has obtained its radiogenic Nd isotope signature (e.g., Jones et al., 2008). While our data support such a mixing hypothesis (blue line in Fig. 8), the major concern with this interpretation is that deep water formation does not happen in the GoA presently. Such downward mixing would be necessary (as opposed to simply upwelling), to transfer more radiogenic εNd signals to depth. A particle-based mechanism to generate these radiogenic εNd signatures at depth is also possible, and in general must account for some fraction of the deep behavior of both [REE] and εNd, as discussed later. However, a particle-based explanation would be expected to shift the εNd signature of deep waters unidirectionally towards more radiogenic values, reflecting the surface water signatures and inputs.

The three hypotheses presented above lead to different implications for the biogeochemical behavior of the REEs and the distribution of εNd in the oceans. Some further insight into this can be found in the surface water data we collected, which appear to reflect the generally radiogenic local Nd input (0 to −2 εNd), but vary widely in concentration. Such concentration variability implies that there is significant biogeochemical cycling of Nd in the surface waters, with important Nd contributions from the shelves. What is surprising is that these surface data also appear to follow a pronounced two-component mixing trend (green line; Fig. 8). The spatial distribution of these surface data (Fig. 5) indicates that the end-members of this mixing are most likely samples closest to the coast (highest Nd concentrations, most positive εNd) and those furthest away in the open gyre (lowest Nd concentrations, most negative εNd). These observations indicate that despite strong biogeochemical processing of elemental Nd in the study area, the Nd isotopes maintain the ability to trace mixing of distinct input sources and surface ocean circulation, a finding previously also noted in across-shelf measurements in the Bering Sea and on the Siberian Shelf (Andersson et al., 2008; Porcelli et al., 2009).

4.2. REEs in the Gulf of Alaska

The interpretation of the REE data is complicated by the challenge of comparing all 14 REEs with other intrinsic oceanographic properties within a complex spatial distribution. Often simplifications and parameterizations facilitate the interpretation of REE data. Here, we have taken this idea further in order to look at the entire REE data set. Our approach was to first evaluate statistically if the pattern groupings estimated by eye (Fig. 4) are robust. To do this, we ran a Q-mode factor analysis on three data manipulations: (1) the measured concentrations; (2) these concentrations normalized to the mean REE within each sample and (3) these mean-normalized concentrations normalized again by the element mean of all samples (Klovan and Imbrie, 1971; Klovan and Miesch, 1976; Klovan, 1981). In all three cases, the factor scores returned fundamentally the same result (results for the third manipulation are given in Tables 1 and 2), indicating that there are two distinct groups of REE patterns in these samples that exist regardless of absolute concentration in the sample and relative concentrations of each REE between all samples. As a fourth analysis, we ran the doubly-normalized (third) data manipulation without the Ce data, given that Ce follows a redox chemistry in seawater different from the other REEs. The factor loading of this fourth data manipulation differs somewhat from the results that include Ce (Tables 1 and 2) but the two patterns seen in the first three analyses

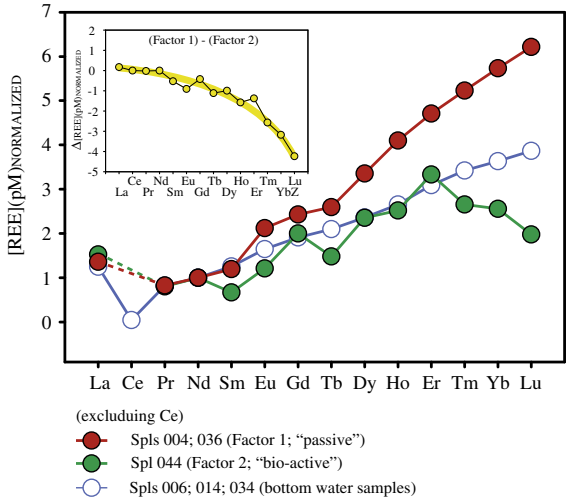

Fig. 9. REE patterns of Factor 1 and Factor 2. These represent the samples most characteristic of the "passive" (Factor 1) and "bio-active" (Factor 2) REEs. The average of the three deepest (bottom water) samples is also shown. *Inset*: the difference between the Factor 1 and Factor 2 patterns: it is hypothesized that the inverse of this pattern should be found in non-dissolved phases associated with microbial activity.

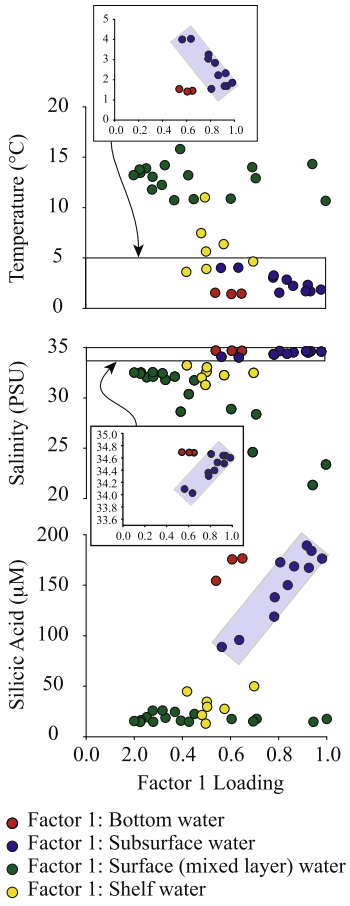

Fig. 10. Factor 1 loadings versus water property. Of the parameters tested, the Factor 1 loadings correlate best between the subsurface water (blue circles) and intrinsic water mass properties. The bottom waters (red circles) differ from the other deep-water samples, indicative of additional processes affecting the bottom waters. (For interpretation of the references to color in this figure legend, the reader is referred to the web version of this article.)

are emphasized and confirmed. From these factor loading results, we isolated the samples that best (i.e., with >0.95 loading of that factor) represented the two factors (which explained >98% of the total variance for all the manipulations analyzed). As shown in Fig. 9, these analyses extracted exactly the two pattern "types" grouped by eye. Therefore, we conclude that it is a robust result that the two types of GoA REEs can be clearly distinguished by their patterns. Again, because concentrations were normalized in these analyses, this conclusion does not relate to the absolute abundances of REEs in a particular sample but only depends on their patterns.

To better understand how these REE patterns are related to a particular process that controlled their fractionation, we compared the factor loadings (which reflect one type of REE pattern only) to the originally measured concentrations in the same samples. While there is some overlap, the samples with >50% Factor 1 loadings are those with the highest REE concentrations (Tables 1 and 2). Moreover, the weightings of this factor in the subsurface waters varies with temperature, salinity and silicic acid (Fig. 10), except for Samples 006, 014 and 034, which are the three bottom water samples analyzed. Considering these characteristics, we argue that while the concentration profiles of Nd, or any other trivalent REE, does not obviously show it, there is a dominant component (>0.8 Factor 1 loadings in most cases) of the REEs that are indeed behaving as "preformed REEs" (i.e., quasi-conservatively) in the deep water samples. It is most likely that these dominant REEs (Factor 1) are those complexed by abundant carbonate ions (Cantrell and Byrne, 1987) and thus behave like a preformed species such as PO_4^* (Broecker et al., 1991; De Souza et al., 2012).

Below the surface, it is only the deepest samples (006, 014 and 034) that deviate from this behavior. The deviation of these bottom water REEs most likely reflects a *loss* from the dissolved phase, based on the factor loadings and by comparison to the dissolved silicic acid concentration. Moreover, the REE patterns of these bottom water samples do not appear particularly HREE depleted (Fig. 9). These data thus imply that there is a benthic sink process, potentially in contradiction to suggestions of a benthic source of REEs (Haley and Klinkhammer, 2003; Haley et al., 2004), or of a zero-loss exchange process (e.g., Lacan and Jeandel, 2005), or a combination of the two. Such a loss-term is consistent with previous observations (Piepgras and Jacobsen, 1988; Grasse et al., 2012), and is consistent with the apparent conservative nature of εNd in the deep ocean. That is, loss of Nd from the dissolved phase (with no associated exchange) at the sea-floor would *not* affect the εNd measured in the bottom water, as discussed previously. We summarize from these observations that there is a dynamic interaction between the sediments, sediment pore waters and overlying waters. However, the mechanism of this interaction still remains an outstanding question in marine REE and Nd isotope research.

There is also a second component of the REEs measured (i.e., Factor 2) that has a distinct pattern (Fig. 9) and appears to behave non-conservatively in the oceans (i.e., does not co-vary with intrinsic seawater properties). While the Factor 2 loadings are generally smaller than Factor 1, the distribution is such that, excepting five samples (001, 003, 004, 024, 023), all of the samples in the upper 100 m have Factor 2 loadings >0.5 (Table 1). The five "anomalous" samples are all found on the northwestern margin of the GoA in coastal waters carrying a high suspended load at the time of sampling (Fig. 1 inset), and will thus be discussed separately below. The difference between the Factor 2 and Factor 1 REEs, generally reflecting the difference in REEs between the surface and subsurface GoA, is most readily described as a progressively intensifying depletion with increasing atomic mass (Fig. 9). This pattern is predicted from models involving particulate scavenging of REEs with preferential HREE depletion in the dissolved phase, and especially those models that invoke organic carbon as the scavenging phase (Byrne and Kim, 1990; Takahashi et al., 2007). We thus argue that the removal of REEs by non-dissolved phases (organic or otherwise) results in surface water REEs with the Factor 2 type pattern. Further, the resulting residual REE pattern in the dissolved phase (i.e., Factor 2) bears many similarities to the REE pattern seen in anoxic pore waters as a consequence of the reduction of iron oxides (Haley et al., 2004), an observation we now explore further.

No obvious correlations were found when comparing the Factor 2 loadings with seawater properties indicative of biologic control (i.e., nitrate, phosphate, silicate, oxygen and chlorophyll-a; Tables 1 and 2; chlorophyll data – not shown – from MODIS and SeaWIFS data at http://oceancolor.gsfc.nasa.gov/). Therefore, it is unlikely that the activity of photosynthetic organisms are driving the processes that control the Factor 2 pattern in surface waters, contrary to previous suggestions (Haley et al., 2005). However, a compelling model for microbial mediation can be set up to explain these surface REEs. Such microbial mediation is known to impact Ce (Moffett, 1990, 1994) but here we suggest that these same microbes also impact all the other REEs. Specifically, microbial siderophores (highly specific Fe-chelating molecules made by organisms for the acquisition and retention of iron; Mawji et al., 2008; Christenson and Schijf, 2011) may account for the removal of dissolved REEs characterized by the HREE-enriched pattern predicted (Fig. 9), not directly as a redox related processes (as is the case for Ce), but simply as an indirect effect of microbial processing of iron. This idea is consistent with the high affinity of the REEs to both iron and organic molecules (Goldberg et al., 1963; Elderfield and Greaves, 1982; Byrne and Kim, 1990; Stanley and Byrne, 1990; Sholkovitz, 1992; Sholkovitz et al., 1992; Arraes-Mescoff et al., 2001; Tang and Johannesson, 2003; Haley et al., 2005; Christenson and Schijf, 2011) and the fact that this type pattern is predominantly found in the mixed layer, even below the photic zone. This also explains why nutrients do not co-vary with the Factor 2 loadings. Moreover, this biogeochemical model can account for the REEs associated with Fe-oxides having a MREE-enriched pattern, as has been observed to be the case (e.g., Gutjahr et al., 2007). That is, if organically bound Fe is associated with heavy-enriched REEs, the residual inorganic Fe (oxides) may be associated with the residual REEs that are relatively MREE-enriched. This hypothesis implies that microbial activity, via iron cycling by siderophore ligands produced by bacteria, has indirect control over the non-conservative REE distribution in the oceans. While these data are not sufficient to comprehensively test this hypothesis, they do provide a potential mechanism that is consistent with and can explain REE dynamics from the oxic ocean surface to deeply anoxic sediments, while not contradicting the observed dissolved Nd isotope distributions.

4.3. A REE/Nd isotope model for the Gulf of Alaska

Taking all of the above observations into consideration, our hypothesis is that there are two pools of REEs: a "passive" pool complexed to carbonate ions and a "bio-reactive" pool altered indirectly through microbial processing of iron oxides and complexed by organic molecules, possibly siderophores (Fig. 11; Christenson and Schijf, 2011). In the subsurface ocean, the REEs behave quasi-conservatively (similar to a "preformed" element), as their Nd isotope compositions suggest. Specifically, our model suggests that both εNd and [REE] are largely intrinsic properties of the water masses and, as such, properties such as HREE/LREE or MREE/MREE* (Table 3) could also be used to trace these water masses. Our model implicitly incorporates the idea that there is particle/water exchanges at depth that helps to transfer signals vertically through the water column (e.g., Sholkovitz et al., 1994), just as happens with other elements that show a preformed behavior. The extent to which a water mass signal is influenced by the "preformed" versus the "remineralized" type (for the REEs, this is more likely to be "exchanged") will need to be investigated further as a test of this hypothesis.

In the surface ocean, neodymium isotope signatures are not fractionated during microbial activity. However, microbially complexed REEs may potentially affect the "bio-reactive" REE pool and its Nd isotopic signature for two reasons: (1) microbial activity may act on iron sources that can carry a Nd isotope signature different from ambient seawater; (2) strong recycling of these "bio-reactive" REEs may increase their apparent surface ocean residence time, and thus through circulation might generate a deviation from ambient seawater mixing relationships over time. Indeed, the coastal Nd concentration and isotope signatures found in the surface waters in the centre of an eddy (Fig. 5) provide evidence in support of both these possibilities. A third reason to expect the "bio-reactive" REEs to carry a distinct Nd isotopic fingerprint is reflected in the impact of pore water or submarine ground water discharge (SGD) on the REE budget of the ocean (Haley et al., 2004; Johannesson and Burdige, 2007). Such an influence would more strongly impact the margins and surface waters of the GoA and would generate distinct Nd isotopic signatures near-shore. Under this umbrella of interfacial (margins and sea floor) interactions falls the possibility of "boundary

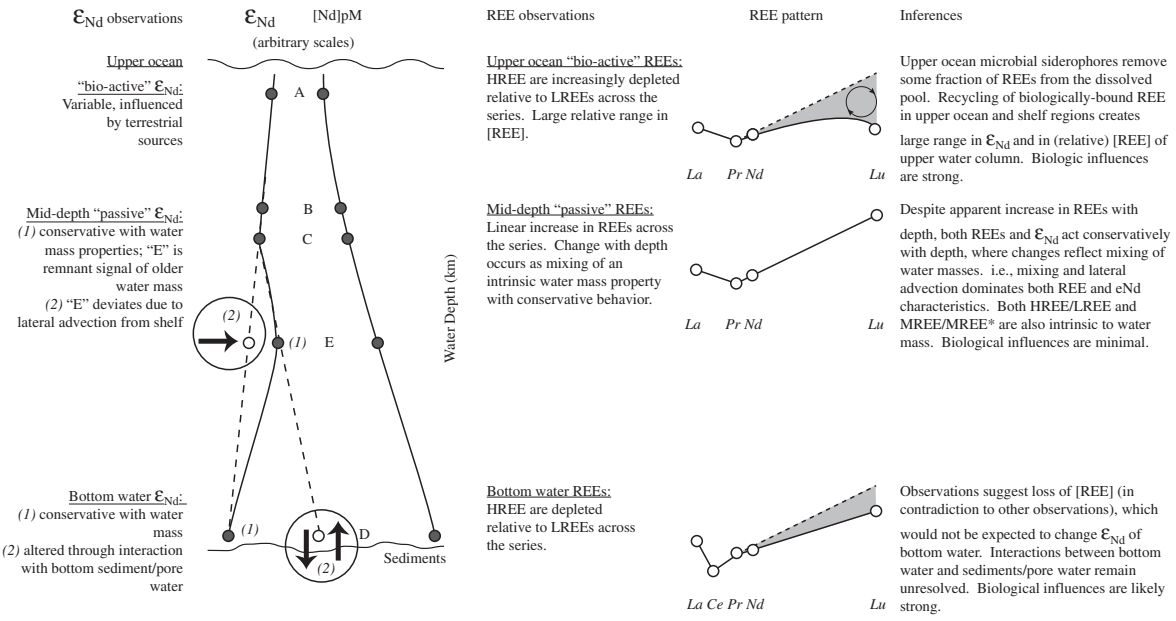

Fig. 11. Summary of the model concept. Our model to explain REEs and εNd in the GoA, based on (left to right): (1) εNd and (2) [REE] profiles (e.g., Nd), and (3) REE patterns. The water column is divided into three sections: the upper water column (above MtW; point A), subsurface water (points B, C and E in Fig. 7) and bottom water (point D). Gray circles represent the profile data observed; when options exist, our best explanation for these data is listed as Option (1). Option (2) is also presented; the shift in εNd described by Option (2) is illustrated by comparing the open circles with the observed (gray) circles. The area of the REE patterns shaded in gray represents the deviation from that of "passive" REEs; i.e., those seen in mid-depths that appear to behave conservatively.

exchange" (Lacan and Jeandel, 2005). The impact of these sediment-based processes needs to account for both the mass balance of the REEs, as well as their Nd isotopic composition. While all the data presented here are consistent with previous Nd isotope data indicative of a loss term into the sediments, they are inconsistent with a sediment REE-source (i.e., pore water or submarine groundwater discharge) as well as a steady-state equilibrium (i.e., boundary exchange) of REEs between the sediments and the water column. In light of the sediment/water interactions at the ocean floor, our data can only serve to highlight this as an outstanding question of marine REE research. Our model does, however, offer an intriguing potential mechanism to explain the conflicting observations of bottom water εNd and [REE], whereby REEs are passively incorporated into biological cycling of nutrient elements. In this model, [REE] may be dramatically affected by biogeochemical processing with little to no associated change in εNd, which may be critical in sediment pore waters that are known to have highly dynamic biogeochemical cycling (e.g., Haley et al., 2004). However, what exactly the biogeochemical processes are that occur in the sediments and that impact the REEs, and how these influence εNd of pore and bottom water is yet to be determined by dedicated sediment pore water studies.

5. CONCLUSIONS

This work presents spatial and depth distributions of dissolved REEs and Nd isotopes across the GoA and for the first time documents the ability of εNd signatures to trace eddies as an important means to carry shelf signatures to open gyre regions. Statistical analyses of the REE patterns reveal two distinct patterns and we present a new conceptual model to describe the distribution of REEs and Nd isotopes in the Gulf of Alaska. Our model is based on REEs in the subsurface ocean being complexed to carbonate ion and largely behaving "quasi-conservatively", consistent with a preformed element. The isotope signatures of this part of the Nd pool trace deep water circulation identical to a preformed nutrient. The subsurface REEs being essentially conservative is consistent with the idea that this far northeastern corner of the Pacific maintains a "pool" of old seawater reflecting processes integrating over the past 1000 years, which is observable in both ^{14}C content and Nd isotope composition, but not as clearly in temperature and salinity. We hypothesize that there is also a "bio-reactive" pool of REEs that is present in all samples, that is only significant in the upper, near surface ocean. We argue that these reactive REEs are complexed by organic molecules, probably siderophores, as a result of microbial processing. As such, this processing would only impact the REEs secondarily through mutual affinity to both Fe and organics. While other processes may impact the Nd isotopic compositions at margins, the distinct signature of near surface water parcels transported by eddies in the Gulf of Alaska indicates that the microbial mediation of REEs proposed here has no direct impact on the distribution of Nd isotopes. However, mixing of Nd from this "bio-reactive" pool with an isotopically distinct "passive" pool of Nd may eventually influence the total Nd isotope signature.

ACKNOWLEDGMENTS

The authors would like to thank the captain and crew of the R/V Thompson, chief scientist Ken Bruland, and the entire scientific party of the cruise, with special thanks to Bettina Sohst for nutrient data. Our deepest appreciation goes to Jutta Heinze and the lab group at GEOMAR for all the help in the lab. Finally, we would like to thank Jorg Rickli and two anonymous reviewers for their comments, and Derek Vance for editorial handling of this manuscript.

REFERENCES

Akagi T., Fu F.-F., Hongo Y. and Takahashi K. (2011) Composition of rare earth elements in settling particles collected in the highly productive North Pacific Ocean and Bering Sea: implications for siliceous-matter dissolution kinetics and formation of two REE-enriched phases. *Geochim. Cosmochim. Acta* **75**, 4857–4876.

Alibo D. S. and Nozaki Y. (1999) Rare earth elements in seawater: particle association, shale-normalization and Ce oxidation. *Geochim. Cosmochim. Acta* **63**, 363–372.

Andersson P. S., Porcelli D., Frank M., Bjork G., Dahlqvist R. and Gustaffson R. (2008) Neodymium isotopes in seawater from the Barents Sea and Fram Strait Arctic–Atlantic gateways. *Geochim. Cosmochim. Acta* **72**, 2854–2867.

Arraes-Mescoff R., Roy-Barman M., Coppola L., Souhaut M., Tachikawa K., Jeandel C., Sempere R. and Yoro C. (2001) The behavior of Al, Mn, Ba, Sr, REE and Th isotopes during in vitro degradation of large marine particles. *Mar. Chem.* **73**, 1–19.

Arsouze T., Dutay J.-C., Lacan F. and Jeandel C. (2009) Reconstructing the Nd oceanic cycle using a coupled dynamical–biogeochemical model. *Biogeoscience* **6**, 2829–2846.

Broecker W. S., Blanton S., Smethie W. M. and Ostlund G. (1991) Radiocarbon decay and oxygen utilization in the deep Atlantic Ocean. *Global Biogeochem. Cycles* **5**, 87–117.

Brown M. T., Lippiatt S. M., Lohan M. C. and Bruland K. W. (2012) Trace metal distributions within a Sitka eddy in the northern Gulf of Alaska. *Limnol. Oceanogr.* **57**, 503–518. http://dx.doi.org/10.4319/lo.2012.57.2.0503.

Bruland K. W., Rue E. L., Smith G. J. and DiTullio G. R. (2005) Iron, macronutrients and diatom blooms in the Peru upwelling regime: brown and blue waters of Peru. *Mar. Chem.* **93**, 81–103.

Byrne R. H. and Kim K.-H. (1990) Rare earth elements scavenging in seawater. *Geochim. Cosmochim. Acta* **54**, 2645–2656.

Byrne R. H. and Sholkovitz E. R. (1996) Marine chemistry and geochemistry of the lanthanides. In *The Handbook on the Physics and Chemistry of the Rare Earths* (eds. , Jr.K. A. Gschneidner and L. Eyring). Elsevier, Amsterdam, The Netherlands, pp. 497–593.

Cantrell K. J. and Byrne R. H. (1987) Rare earth element complexation by carbonate and oxalate ions. *Geochim. Cosmochim. Acta* **51**, 597–605.

Carter P., Vance D., Hillenbrand C. D., Smith J. A. and Shoosmith D. R. (2012) The neodymium isotopic composition of waters masses in the eastern Pacific sector of the Southern Ocean. *Geochim. Cosmochim. Acta* **79**, 41–59.

Christenson E. A. and Schijf J. (2011) Stabilty of YREE complexes with the trihydroxamate siderophore desferrioxamine B at seawater ionic strength. *Geochim. Cosmochim. Acta* **75**, 7047–7062.

De Souza G. F., Reynolds B. C., Rickli J., Frank M., Saito M., Gerringa L. J. A. and Bourdon B. (2012) Southern Ocean control of silicon stable isotope distribution in the deep Atlantic Ocean. *Global Biogeochem. Cycles* **26**, GB2035. http://dx.doi.org/10.1029/2011GB004141.

Elderfield H. (1988) The oceanic chemistry of the rare-earth elements. *Philos. Trans. R. Soc. Lond.* **325**, 105–126.

Elderfield H. and Greaves M. J. (1982) The rare earth elements in seawater. *Nature* **296**, 214–219.

Elderfield H., Upstill Goddard R. and Sholkovitz E. R. (1990) The rare-earth elements in rivers, estuaries, and coastal seas and their significance to the composition of ocean waters. *Geochim. Cosmochim. Acta* **54**, 971–991.

Frank M. (2002) Radiogenic isotopes: tracers of past ocean circulation and erosional input. *Rev. Geophys.* **40**, 1001. http://dx.doi.org/10.1029/2000RG000094.

Goldberg E. D., Koide M., Schmitt R. A. and Smith R. H. (1963) Rare-earth distributions in the marine environment. *J. Geophys. Res.* **68**, 4209–4217.

Goldstein S. L. and Hemming S. H. (2003) Long lived isotopic tracers in oceanography, paleoceanography, and ice sheet dynamics. In *Treatise on Geochemistry* (ed. H. Elderfield). Elsevier, New York, pp. 453–489.

Grasse P., Stichel T., Stumpf R., Stramma L. and Frank M. (2012) The distribution of neodymium isotopes and concentrations in the Eastern Equatorial Pacific: water mass advection versus particle exchange. *Earth Planet. Sci. Lett.* **353**, 198–207.

Gutjahr M., Frank M., Sterling C. H., Klemm V., van de Flierdt T. and Halliday A. N. (2007) Reliable extraction of a deepwater trace metal isotope signal from Fe–Mn oxyhydroxide coatings of marine sediments. *Chem. Geol.* **242**, 351–370.

Haley B. A. and Klinkhammer G. P. (2003) Complete separation of rare earth elements from small volume seawater samples by automated ion chromatography: method development and application to benthic flux. *Mar. Chem.* **82**, 197–220.

Haley B. A., Klinkhammer G. P. and McManus J. (2004) Rare earth elements in pore waters of marine sediments. *Geochim. Cosmochim. Acta* **68**, 1265–1279.

Haley B. A., Klinkhammer G. P. and Mix A. C. (2005) Revisiting the rare earth elements in foraminiferal tests. *Earth Planet. Sci. Lett.* **239**, 79–97.

Hathorne E. C., Haley B., Stichel T., Grasse P., Zieringer M. and Frank M. (2012) Online preconcentration ICP-MS analysis of rare earth elements in seawater. *Geochem. Geophys. Geosyst.* **13**, Q01020. http://dx.doi.org/10.1029/2011GC003907.

Henderson G. M. et al. (2007) GEOTRACES – an international study of the global marine biogeochemical cycles of trace elements and their isotopes. *Chem. Erde: Geochem.* **67**, 85–131.

Jacobsen S. B. and Wasserburg G. J. (1980) Sm–Nd isotopic evolution of chondrites. *Earth Planet. Sci. Lett.* **50**, 139–155.

Jeandel C., Arsouze T., Lacan F., Techine P. and Dutay J. C. (2007) Isotopic Nd composition and concentrations of the lithogenic inputs into the ocean: a compilation, with emphasis on the margins. *Chem. Geol.* **239**, 156–164.

Johannesson K. H. and Burdige D. J. (2007) Balancing the global oceanic neodymium budget: evaluating the role of groundwater. *Earth Planet. Sci. Lett.* **253**, 129–142.

Jones K. M., Khatiwala S. P., Goldstein S. L., Hemming S. R. and vande Flierdt T. (2008) Modeling the distibution of Nd isotopes in the coceans using an ocean general circulation model. *Earth Planet. Sci. Lett.* **272**, 610–619.

Klovan J. E. (1981) A generalization of extended Q-Mode factor analysis to data matrices with variable row sums. *Math. Geol.* **13**(3), 217–224.

Klovan J. E. and Imbrie J. (1971) An algorithm and FORTRAN-IV program for large-scale Q-Mode factor analysis and calculation of factor scores. *Math. Geol.* **3**(1), 61–77.

Klovan J. E. and Miesch A. T. (1976) Extended CABFAC and QMODEL computer programs for Q-mode factor analysis of compositional data. *Comput. Geosci.* **1**(3), 161–178.

Lacan F. and Jeandel C. (2001) Tracing Papua New Guinea imprint on the central Equatorial Pacific Ocean using neodymium isotopic compositions and Rare Earth Element patterns. *Earth Planet. Sci. Lett.* **186**, 497–512.

Lacan F. and Jeandel C. (2005) Neodymium isotopes as a new tool for quantifying exchange fluxes at the continent–ocean interface. *Earth Planet. Sci. Lett.* **232**, 245–257.

Ladd C., Stabeno P. and Cokelet E. D. (2005) A note on cross-shelf exchange in the northern Gulf of Alaska. *Deep Sea Res. II* **52**, 667–679.

Ladd C., Crawford W. R., Harpold C. E., Johnson W. K., Kachel N. B., Stabeno P. J. and Whitney F. (2009) A synoptic survey of young mesoscale eddies in the Eastern Gulf of Alaska. *Deep Sea Res. II* **56**, 2460–2473.

Laes A., Blan S., Laan P., Achterberg E. P., Sarthou G. and de Baar H. J. W. (2003) Deep dissolved iron profiles in the eastern North Atlantic in relation to water mass. *Geophys. Res. Lett.* **30**, 1902. http://dx.doi.org/10.1029/2003GL017902.

Lippiatt S. M., Lohan M. C. and Bruland K. W. (2010) The distribution of reactive iron in northern Gulf of Alaska coastal waters. *Mar. Chem.* **121**, 187–199.

Mawji E., Gledhill M., Milton J. A., Tarran G. A., Ussher S., Thompson A., Wolff G. A., Worsfold P. J. and Achterberg E. P. (2008) Hydroxamate siderophores: occurrence and importance in the Atlantic Ocean. *Environ. Sci. Technol.* **42**, 8675–8680.

Miura T., Suga T. and Hanawa K. (2002) Winter mixed layer and formation of dichothermal water in the Bering Sea. *J. Oceanogr.* **58**, 815–823.

Moffett J. W. (1990) Microbially mediated cerium oxidation in seawater. *Nature* **345**, 421–423.

Moffett J. W. (1994) A radiotracer study of cerium and manganese uptake onto suspended particles in Chesapeake Bay. *Geochim. Cosmochim. Acta* **58**, 695–703.

Murphy K. and Dymond J. (1984) Rare earth element fluxes and geochemical budget in the eastern equatorial Pacific. *Nature* **307**, 444–447.

Nance W. B. and Taylor S. R. (1976) Rare-earth element patterns and crustal evolution. 1. Australian post-Archean sedimentary rocks. *Geochim. Cosmochim. Acta* **40**, 1539–1551.

Ngwenya B. T., Magennis M., Olive V., Mosselmans J. F. W. and Ellam R. M. (2010) Discrete site surface complexation constants for lanthanide adsorption to bacteria as determined by experiments and linear free energy relationships. *Environ. Sci. Technol.* **44**, 650–656.

Nudds S. H. and Shore J. A. (2011) Simulated eddy induced vertical velocities in a Gulf of Alaska model. *Deep Sea Res. I* **58**, 1060–1068.

Piepgras D. J. and Jacobsen S. B. (1988) The isotopic composition of neodymium in the North Pacific. *Geochim. Cosmochim. Acta* **52**, 1373–1381.

Pin C. and Zalduegui J. F. S. (1997) Sequential separation of light rare-earth elements, thorium and uranium by miniaturized extraction chromatography: application to isotopic analyses of silicate rocks. *Anal. Chim. Acta* **339**, 79–89.

Porcelli D., Andersson P. S., Baskaran M., Frank M., Bjork G. and Semiletov I. (2009) The distribution of neodymium isotopes in Arctic Ocean basins. *Geochim. Cosmochim. Acta* **73**, 2645–2659.

Rempfer J., Stocker T. F., Joos F., Dutay J.-C. and Siddall M. (2011) Modelling Nd-isotopes with a coarse resolution ocean circulation model: sensitivities to model parameters and source/sink distributions. *Geochim. Cosmochim. Acta* **75**, 5927–5950.

Rickli J., Frank M., Baker A. R., Aciego S., de Souza G., Georg R. B. and Halliday A. N. (2010) Hafnium and neodymium isotops in surface waters of the eastern Atlantic Ocean: implications for sources and inputs of trace metals to the ocean. *Geochim. Cosmochim. Acta* **74**, 540–557.

Sholkovitz E. R. (1992) Chemical evolution of rare earth elements: fractionation between colloidal and solution phases of filtered river water. *Earth Planet. Sci. Lett.* **114**, 77–84.

Sholkovitz E. R. (1993) The geochemistry of rare earth elements in the Amazon River estuary. *Geochim. Cosmochim. Acta* **57**, 2181–2190.

Sholkovitz E. R. and Szymczak R. (2000) The estuarine chemistry of rare earth elements: comparison of the Amazon, Fly, Sepik and the Gulf of Papua systems. *Earth Planet. Sci. Lett.* **179**, 299–309.

Sholkovitz E., Shaw T. J. and Schneider D. L. (1992) The geochemistry of rare earth elements in the seasonally anoxic water column and porewaters of Chesapeake Bay. *Geochim. Cosmochim. Acta* **56**, 3389–3402.

Sholkovitz E. R., Landing W. M. and Lewis B. L. (1994) Ocean particle chemistry: the fractionation of rare earth elements between suspended particles and seawater. *Geochim. Cosmochim. Acta* **58**, 1567–1579.

Siddall M., Khatiwala S., Van de Flierdt T., Jones K., Goldstein S. L., Hemming S. R. and Anderson R. F. (2008) Towards explaining the Nd paradox using reversible scavenging and the Transport Matrix Method. *Earth Planet. Sci. Lett.* **274**, 448–461.

Singh S. P., Singh S. K., Goswami V., Bhushan R. and Rai V. K. (2012) Spatial distribution of dissolved neodymium and εNd in the Bay of Bengal: role of particulate matter and mixing of water masses. *Geochim. Cosmochim. Acta* **94**, 38–56.

Sonke J. E. and Salters V. J. M. (2006) Lanthanide–humic substances complexation. I. Experimental evidence for a lanthanide contraction effect. *Geochim. Cosmochim. Acta* **70**, 1495–1506.

Stanley, Jr., J. K. and Byrne R. H. (1990) The influence of solution chemistry on REE uptake by *Ulva lactuaca* L. in seawater. *Geochim. Cosmochim. Acta* **54**, 1587–1596.

Stichel T., Frank M., Rickli J. and Haley B. A. (2012a) The hafnium and neodymium isotope composition of seawater in the Atlantic sector of the Southern Ocean. *Earth Planet. Sci. Lett.* **317–318**, 282–294.

Stichel T., Frank M., Rickli J., Hathorne E. A., Haley B. A., Jeandel C. and Pradoux C. (2012b) Sources and input mechanisms of hafnium and neodymium in surface waters of the Atlantic sector of the Southern Ocean. *Geochim. Cosmochim. Acta* **94**, 22–37.

Tachikawa K., Jeandel C., Vangriesheim A. and Dupre B. (1999) Distribution of rare earth elements and neodymium isotopes in suspended particles of the tropical Atlantic Ocean (EUMELI site). *Deep-Sea Res.* **I**(46), 733–755.

Takahashi Y., Chatellier X., Hattori K. H., Kato K. and Fortin D. (2005) Adsorption of rare earth elements onto bacterial cell walls and its implication for REE sorption onto natural microbial mats. *Chem. Geol.* **219**, 53–67.

Takahashi Y., Hirata T., Shimizu H., Ozaki T. and Fortin D. (2007) A rare earth element signature of bacteria in natural waters?. *Chem. Geol.* **244** 569–583.

Talley L. D. (2007) Hydrographic atlas of the world ocean circulation experiment (WOCE). In *Pacific Ocean*, vol. 2 (eds. M. Sparrow, P. Chapman and J. Gould). International WOCE Project Office, Southampton, UK, ISBN 0-904175-54-5.

Talley L. D., Pickard G. L., Emery W. J. and Swift J. H. (2011) *Descriptive Physical Oceanography. An Introduction*, 6th ed. Academic Press, London, ISBN 978-0-7506-4552-2.

Tanaka T., Togashi S., Kamioka H., Amakawa H., Kagami H., Hamamoto T., Yuhara M., Orihashi Y., Yoneda S., Shimizu H., Kunimaru T., Takahashi K., Yanagi T., Nakano T., Fujimaki H., Shinjo R., Asahara Y., Tanimizu M. and Dragusanu C. (2000) JNdi-1: a neodymium isotopic reference in consistency with LaJolla neodymium. *Chem. Geol.* **168**, 279–281.

Tang J. and Johannesson K. H. (2003) Speciation of rare earth elements in natural terrestrial waters: assessing the role of dissolved organic matter from the modeling approach. *Geochim. Cosmochim. Acta* **67**, 2321–2339.

Van de Flierdt T., Pahnke K. and GEOTRACES Intercalibration Participants (2012) GEOTRACES intercalibration of neodymium isotopes and rare earth element concetnrations in seawater and suspended particles. Part 1: reproducibilitiy of results for the international intercomparison. *Limnol. Oceanogr. Methods* **10**, 234–251.

Associate editor: Derek Vance